



Petrogenesis of bismuth minerals in the Dabaoshan Pb–Zn polymetallic massive sulfide deposit, northern Guangdong Province, China



Lin Ye^{a,*}, Tiegeng Liu^a, Yulong Yang^{a,b}, Wei Gao^{a,b}, Ziping Pan^{a,c}, Tan Bao^{a,b}

^a State Key Laboratory of Ore Deposit Geochemistry, Institute of Geochemistry, Chinese Academy of Sciences, Guiyang 550002, China

^b Graduate School of Chinese Academy of Sciences, Beijing 100039, China

^c Geological Survey of Guizhou Province, Guiyang 550004, China

ARTICLE INFO

Article history:

Received 26 November 2012

Received in revised form 2 December 2013

Accepted 4 December 2013

Available online 14 December 2013

Keywords:

Bismuth minerals

Native bismuth

Paragenesis mineralogy

Pb–Zn polymetallic massive sulfide deposit

Dabaoshan

Guangdong

ABSTRACT

Located in the northern Guangdong Province, the Dabaoshan Pb–Zn polymetallic massive sulfide deposit is one of the most important regions to have produced Fe, Cu, Pb, Zn and S in southern China. While much progress has been made with respect to the geology and geochemistry of the deposit, a better understanding of ore genesis is warranted. This ore body contains abundant bismuth element, only few studies exist on the distribution characteristics and existing states of bismuth. Electron microprobe study yields that native bismuth, tellurides (e.g. hedleyite) and sulfide minerals, are the main forms in which this element is found. The occurrence and characteristics of native bismuth and its mineral assemblages are different with high-T gold-bearing deposits, but are more similar to those of mid-low temperature hydrothermal deposits. Our research shows that the Bi(Te) at Dabaoshan derived from the Late Yanshanian dacite porphyry. The Bi(Te)-rich ore-forming fluid developed during intrusion of the dacite and mineralized along fractures, and overprint the earlier Pb–Zn mineralization. During the early overprinting event, the ore-forming fluid was rich in Bi and Te and poor in S, under uniform mid-temperature conditions. As the hydrothermal fluids evolved, they became enriched with Ag and Pb. Sulfur was rich in the fluid during the late overprinting event; this may have been related to dissolution of sulfide. The low abundances of Bi, Te and Ag in sulfide minerals (e.g., galena and sphalerite), indicate that ore genesis and the ore-forming materials were different between the Pb–Zn and Bi–Te–Ag stages. Thus, new geological and geochemical data were used to delineate the sequence ore genesis of Dabaoshan Pb–Zn mineralization.

© 2013 Elsevier Ltd. All rights reserved.

1. Introduction

The Dabaoshan Pb–Zn polymetallic massive sulfide deposit, northern Guangdong province, is one of the most important mineral resources for iron, copper, lead, zinc, and sulfur in southern China with a reserve of approximately 100 Mt of Fe, 0.88 Mt Cu and 1.5 Mt of Pb + Zn. The Dabaoshan deposit is characterized by varied mineral suites and multiple types of mineralization. These include centrally-located (weathering–leaching) iron deposits, volcanic–sedimentary hydrothermal superimposed siderite deposits; northern district porphyry type and skarn type Wo–Mo deposits; and southern district lead–zinc–copper deposits (Fig. 1a).

Substantial progress has been made in studies of the geology and geochemistry of the deposit (e.g. Wang, 2006). Nevertheless, there has been much debate concerning the genesis and ore-forming

mechanisms. As a result, a number of different genetic models have been proposed. Interpretations include: (1) porphyry or continental subvolcanic type deposits (e.g. Gu et al., 1984; Liu et al., 1985); (2) magmatic–hydrothermal type deposits (e.g. Huang et al., 1987; Xu, 2008b); and (3) volcanic-associated massive sulfide (VHMS) (e.g. Chen, 1985; Ge and Han, 1986; Yang, 1997; Gu et al., 2007). It is nevertheless clear from the previous geological and geochemical research that ore formation was a complex, multi-stage process and the observed features cannot be explained by a single metallogenetic model (e.g. Qiu, 1981; Deng et al., 2005; Song et al., 2007).

Lead, zinc, copper, and sulfur are the dominant commodities in the Dabaoshan deposit. Bismuth is an abundant minor element and its presence at significant concentrations has been documented by many previous workers. There is, however, a marked gap in understanding the mineralogical distribution and speciation of bismuth in the deposit. As an important metal, Bi is obtained mainly as a by-product in the gold deposits (e.g. Drummond and Ohmoto, 1985; Chen et al., 2001; Tuomo and Randolph, 2005) and mid-high temperature magmatic hydrothermal deposits (e.g. Newberry, 1998; Simmons, 2001; Barkov et al., 2008), and few of them come

* Corresponding author. Address: State Key Laboratory of Ore Deposit Geochemistry, Institute of Geochemistry, Chinese Academy of Sciences, Guanshui Road 46#, Nanming District, Guiyang 550002, Guizhou Province, China. Tel.: +86 8515895591; fax: +86 8515891664.

E-mail address: yelin@vip.gyig.ac.cn (L. Ye).

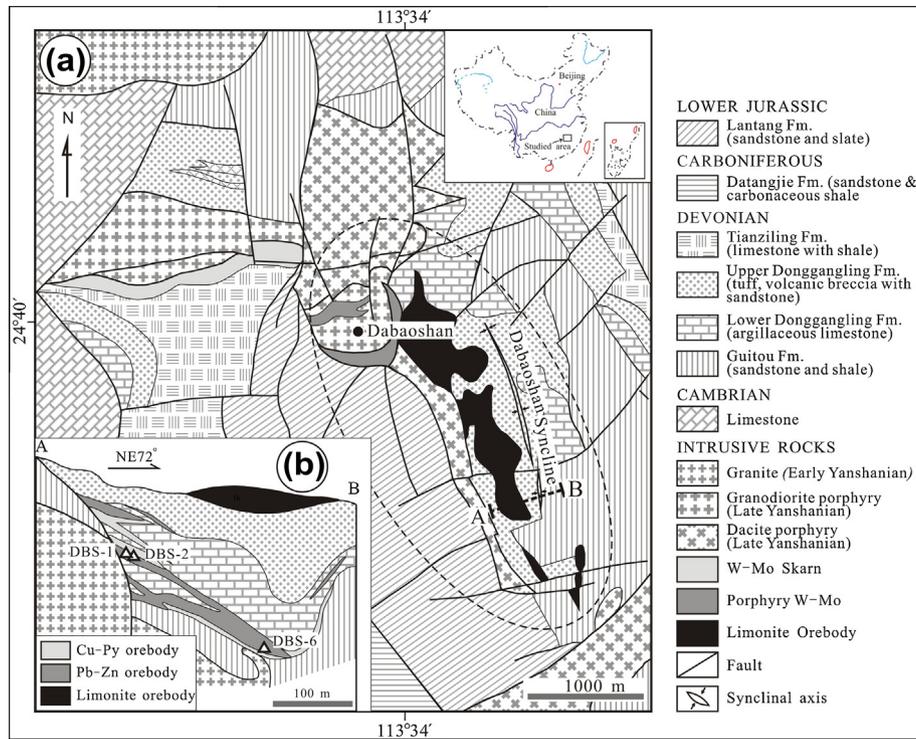


Fig. 1. Geological map (a) and profile map (b) of the Dabaoshan Pb-Zn polymetallic mine, Guangdong (after Wang, 2006).

from middle temperature sulfide deposits (Wang et al., 1982). In this paper, native bismuth and other Bi minerals are described. The occurrence of bismuth in the Dabaoshan deposit is shown to be distinct from that in high temperature hydrothermal deposits. Using the information from the detailed study of bismuth mineralogy, new ideas can be proposed regarding the genesis of the deposit. The classification standard of ore-forming temperature is based on Tu et al. (2003), and the high-, mid- and low temperature means $>300\text{ }^{\circ}\text{C}$, $200\text{--}300\text{ }^{\circ}\text{C}$ and $<200\text{ }^{\circ}\text{C}$ respectively in the paper.

2. Regional geological setting and mineral deposits in the Dabaoshan

The Dabaoshan deposit is located with a plunge of the north-eastern Xueshangzhang anticlinorium in the Neocathaysian structural system. Structurally, the deposit lies at the intersection of the Dadongshan–Guidong E–W-trending structural belt and the Beijiang fault belt in the Shanguan–Wuchuan deep fault belt of the northern Guangdong Paleozoic depression zone (Ge and Han, 1986; Wang, 2006). The N- and NW-trending Dabaoshan syncline ($\sim 2\text{ km}$ in length) is the dominant regional fold in the area of the deposit. It dips at a relatively high angle to the east ($60\text{--}70^{\circ}$), and at $40\text{--}50^{\circ}$ to the west (Fig. 1a). Major faults include N- and NW-trending fault (F_a ; Dabaoshan fault), a NE-trending fault (F_b), and an EW-trending fault. The Dabaoshan fault is closely related to the Pb–Zn mineralization; both F_1^a and F_3^a appear to confine the Dabaoshan deposit.

Exposed rocks in the mine district include terrigenous clastic sedimentary sequences and coast–shallow marine carbonates of the Upper Paleozoic (Early Devonian) epi-metamorphic rock series, and intermediate–acidic lavas and sub-volcanic clastic sedimentary rocks associated with Mid-Devonian seafloor volcanic activity. These strata account for $\sim 70\%$ of surface outcrop across the ore district; minor Early Paleozoic strata are exposed in the northern ore-area. The Mid-Devonian Donggangling Formation is the dominant host for mineralization. It can be sub-divided into: the upper

sub-formation (D_{2d}^b), which is chiefly composed of sandy shale, tuffs, and volcanoclastic breccias, and is marked by the pyritization and siderite mineralization; and the lower sub-formation (D_{2d}^a), which mainly consists of carbonaceous mudstone, mudstone, dolomite, and dolomitic and calcitic sandy shale. The Pb–Zn–Cu orebodies are hosted in the lower sub-formation.

Large volumes of intrusive rocks are closely associated with mineralization. The main intrusions are Yanshanian intermediate–acidic sub-dacite and granitic–dioritic porphyries. Based on geochemical criteria, the pluton is an intermediate–acidic, calc-alkaline, Si–Al-supersaturated intrusive rock, which is K_2O -rich, poor in Na_2O and CaO , and is spatially related to Pb–Zn mineralization (Wang, 2006). The granitic–dioritic porphyries (180–170 Ma, Wang et al., 2010) are found in the northwestern part of the Dabaoshan mine area (Fig. 1a), and are closely associated with Mo mineralization (Wang, 2006). The sub-dacite porphyries are the Dabaoshan dike, and the Jiuquling, Jimatou, and Xuwu intrusions (Fig. 1a), with K–Ar age estimates of 143 Ma (Wang, 2006). There are also minor amounts of diabase and felsite; they formed later than that of Yanshanian intrusions.

Most Cu–sulfide and Pb–Zn polymetallic orebodies occur in the northern and southern parts of the Dabaoshan mine area, respectively. The Pb–Zn segment is 3.1 km long from north to south, 400 m wide (E–W) and outcrops over an area of about 0.36 km^2 . The Pb–Zn orebodies are hosted by carbonate strata of the lower sub-formation of the Donggangling Formation (D_{2d}^a), occur sub-parallel to host-rock bedding, and are situated within 500 m of the eastern part of a sub-dacitic porphyry dike and the hanging wall of the F_3^a fault. The ores are overlain by the upper sub-formation of the Donggangling Formation (D_{2d}^b), which hosts a number of stratiform siderite deposits. A sizeable siderite gossan is exposed at the surface. There are more than 40 individual stratiform, stratoid, lenticular Pb–Zn orebodies. Most Pb–Zn orebodies coexisted with a copper–sulfur orebody, composed of three main polymetallic orebodies (Fig. 1b). The largest Pb–Zn orebody (no. 2/1-w) strikes N–S over a length of 810 m, is 60–210 m wide and 2–35 m in thickness. The next largest (no. 4/16) is 65–100 wide, 5–33 m thick and

extends N-S for about 330 m. The Pb–Zn reserve within these two orebodies contributes nearly 60% of the total Pb–Zn reserves at Dabaoshan.

In addition to the above stratabound deposits, the Dabaoshan porphyry type W–Mo mineralization occurs in the inner and outer contact zone of the Dabaoshan–Chuandu granitic–dioritic porphyry, displaying an annular distribution around the intrusion.

Sphalerite, galena, pyrite, pyrrhotite, and chalcopyrite are the main ore minerals. Gangue minerals are chiefly quartz, chlorite, sericite, and calcite. Ores may be massive to semi-massive, banded, lamellar and disseminated or occur as stringer veins. Ore textures include colloidal, subhedral, anhedral, droplet, inclusion grain, metasomatic corrosion, metasomatic relict and secondary graphic types (Ye et al., 2011). Although Pb (2.34%), Zn (5.19%) and subordinate Cu (0.39%) are the main economic components in the deposit, several minor elements are also present at relatively high concentrations. These include Ag, Bi, Cd, Ga and In; average grades are 61.9 g/t Ag, 0.04% Bi and 180 g/t In, respectively. Wall rock alteration is dominantly represented by skarn (diopside–tremolite–actinolite), sericitization, decoloration, hornfels, epidotization, and silicification.

3. Sampling and analytical methods

The studied samples were collected from Pb–Zn orebody 2/1-w in the southern part of the mine district. Ore mineral assemblages include sphalerite, galena, pyrite and chalcopyrite, with Bi-minerals included in the sulfides. Reflected light microscopy shows a paragenetic sequence of pyrite → galena (early generation)–sphalerite → chalcopyrite → native bismuth → Bi-sulfides → galena (late generation). Native bismuth generally occurs as irregular grains, ranging in size from 0.5 μm to 15 μm, rarely as much as 20 μm. It is altered by late generation galena occurring in the fractures of sphalerite.

Systematic studies of the speciation and distribution of bismuth were performed at the State Key Laboratory of Ore Geochemistry, Institute of Geochemistry, Chinese Academy of Sciences, using a Shimadzu EPMA-1600 electron microprobe equipped with an energy-dispersive spectrometer and back-scatter electron imaging capability. BSE analyses for these samples were conducted on a Shimadzu EPMA-1600 electron probe. Operating conditions for investigation of mineral phases were 1000–4000× magnification, accelerating voltage of 25 kV, and beam current of 4.5 nA. Instrument conditions were: 25 kV accelerating voltage, 20 nA beam current, 1 μm electron beam spot diameter, and 100 s count times for unknown or background. SPI standards were used, and the minimum detection limits of Bi, Ag, As, Zn, Fe, Pb, Cd, Cu, S and Te are 0.1%. The selected analytical spectral lines and deducted background values were achieved using instrument programs, and some fault spectral peaks were calibrated artificially. All related analytical processes were made using the method of Tu et al. (2003) and performed at IG-CAS, Guiyang. All data are given in terms of weight percent in the paper.

4. Results

Electron microprobe and energy spectra analytical data are presented in Table 1, Appendix 1 and illustrated in Fig. 2.

4.1. Bismuth minerals

Bismuth occurs within a number of discrete Bi-minerals in the Pb–Zn ores, including native bismuth. Their paragenesis and compositions are described here.

4.1.1. Native bismuth

Native bismuth is the dominant mode of occurrence of Bi. The mineral exhibits a variety of textures: (1) alteration by galena which formed in the late mineralization stage (Fig. 2a–b, Appendix 1); (2) partly overprinting early generation galena and sometimes coexisting with it (Fig. 2c, Appendix 1); and (3) anhedral crystals and veinlets hosted along fractures or vugs within sphalerite. Native bismuth is fine-grained, reaching a maximum size of 15 × 20 μm. EDAX analysis indicates the presence of various amounts of different trace elements such as Ag (up to 2.99%, respectively); S and Te were not identified at concentrations above minimum detection limits. A few of the analyzed grains were marked by a fluorine peak corresponding to as much as 1.93%.

4.1.2. Hedleyite

Minerals of the tetradymite group are widespread as micron-sized inclusions in the sulfides from Dabaoshan. These minerals occur as coarse anhedral grains (5 × 8 μm to 10 × 30 μm) along cracks and vugs in the sphalerite, enclosed by early generation galena (Fig. 2d) or chalcopyrite (Fig. 2e), and partly associated with Ag–Te–S or Ag–Bi–Pb–S minerals, or overprinted by these minerals and occurring as veinlets. The dispersive energy spectra show distinct Bi and Te peaks. Bi and Te contents of this Bi–Te mineral vary from 72.44% to 82.31% with an average of 78.13% and from 17.69% to 27.55% with an average of 22.38%, respectively ($n = 8$, Table 1 and Appendix 1). The minerals are devoid of S and Pb. The atomic percent ratio of Bi and Te is close to 7:3, which is correspondingly close to $\text{Bi}_{6.42}\text{Te}_3$ (Appendix 1), expressed simply as Bi_7Te_3 . Its composition is consistent with that of hedleyite (Bi_7Te_3 : Bi of 76.61 wt%, Te of 23.39 wt%; Criddle and Stanley, 1993; Ciobanu et al., 2010). The Bi/Te ratio of the analyzed phase is appreciably higher than that of tellurobismuthite, Bi_2Te_3 (e.g., Criddle and Stanley, 1993). Tellurobismuthite is a relatively common mineral and its formula well known (e.g., Ciobanu et al., 2009; Cook et al., 2007b).

4.1.3. Bismuthinite

Bismuthinite were observed rarely, and where seen, occurred as finer grained amorphous veinlets overprinting early generation galena (Fig. 2f) and other Bi-minerals. These Bi-bearing sulfides mainly contain Bi and S (81.92% and 18.08%, respectively, Table 1 and Appendix 1), and are deficient in Te, Ag and Pb. The atomic percent ratio of Bi and S is close to 2:3, and can be calculated as $\text{Bi}_{2.09}\text{S}_3$, represented by the simple formula Bi_2S_3 . The S and Bi content of the mineral is similar with that of bismuthinite (Bi_2S_3 ; Criddle and Stanley, 1993).

4.1.4. Bi–Ag–Te–S minerals

The Bi–Ag–Te–S minerals are present in minor quantities. Most of them are cubic crystals ($\pm 8 \times 8 \mu\text{m}$), coexisting with late generation galena and enclosed by Ag–Pb–Te–S as minute inclusions (Fig. 2g). The BSE image shows that the type mineral is not a mixture. The Bi, Ag, Te and S contents in this mineral are $21.27 \pm 0.34\%$, $47.09 \pm 0.06\%$, $25.08 \pm 0.25\%$ and $6.56 \pm 0.03\%$ (Table 1 and Appendix 1), respectively, and the mineral is devoid of Pb and Au. The mineral composition can be calculated as $\text{Ag}_{4.22}\text{Bi}_{0.96}\text{Fe}_{0.22}\text{Te}_{1.88}\text{S}_2$, which may be simply expressed as $\text{Ag}_4\text{BiTe}_2\text{S}_2$. Its composition is different from buckhornite ($\text{AuPb}_2\text{BiTe}_2\text{S}_3$; Francis et al., 1992) and empressite (AgTe ; Cipriani, 2004), and resembles Kurilite, or $(\text{Ag,Au})_2(\text{Te,Se,S})$, with Ag content of 44.48%, Te of 21.05%, Au of 27.08%, Se of 6.51%, and S of 0.88%; Criddle and Stanley, 1993), but contains Bi and has a scarcity of Au and Se. It may be a mineral between volynskite (AgBiTe_2) and matildite (AgBiS_2).

4.1.5. Bi–Pb–Te–S minerals

Bi–Pb–Te–S minerals are rare. They occur as anhedral grains ($\pm 10 \times 20 \mu\text{m}$ in size) along cracks or lining vugs within sphalerite

Table 1
EPMA and energy spectrum analysis of selected minerals (%).

| Mineral | Formula | | Number of analyses | Bi | Ag | Te | S | Pb | Zn | Fe | Cu | Cd | F |
|-------------------------------|---|------|--------------------|--------|-------|-------|-------|-------|-------|-------|-------|------|------|
| Native bismuth | Bi | Mean | 20 | 99.67 | 1.08 | – | – | – | – | – | – | – | – |
| | | S.D. | | 0.80 | 1.30 | – | – | – | – | – | – | – | – |
| | | Min | | 97.01 | – | – | – | – | – | – | – | – | – |
| | | Max | | 100.00 | 2.99 | – | – | – | – | – | – | – | 1.93 |
| Hedleyite | Bi _{6.42} Te ₃ | Mean | 8 | 78.13 | – | 22.38 | – | – | – | – | – | – | – |
| | | S.D. | | 3.84 | – | 3.86 | – | – | – | – | – | – | – |
| | | Min | | 72.44 | – | 17.69 | – | – | – | – | – | – | – |
| | | Max | | 82.31 | – | 27.55 | – | – | – | – | – | – | – |
| Bismuthinite | Bi _{2.09} S ₃ | | 1 | 81.92 | – | – | 18.08 | – | – | – | – | – | |
| Bi–Ag–Te–S undefined minerals | (Bi _{0.50} Ag _{2.13})(Te _{0.96} S) | Mean | 2 | 21.27 | 47.09 | 25.08 | 6.56 | – | – | – | – | – | – |
| | | S.D. | | 0.34 | 0.06 | 0.25 | 0.03 | – | – | – | – | – | |
| | | Min | | 21.03 | 47.05 | 24.90 | 6.54 | – | – | – | – | – | |
| | | Max | | 21.51 | 47.13 | 25.26 | 6.58 | – | – | – | – | – | |
| Bi–Pb–Te–S undefined minerals | (Bi _{0.71} Pb _{0.83})(Te _{0.40} S) | | | 36.57 | – | 12.68 | 7.95 | 42.81 | – | – | – | – | |
| Ag–Pb–Bi–S undefined minerals | Pb _{2.15} Bi _{2.80} Ag _{0.91} S ₅ | Mean | 3 | 45.41 | 7.65 | – | 12.44 | 34.50 | – | – | – | – | – |
| | | S.D. | | 1.10 | 0.24 | – | 0.13 | 0.85 | – | – | – | – | – |
| | | Min | | 44.14 | 7.49 | – | 12.30 | 33.92 | – | – | – | – | – |
| | | Max | | 46.07 | 7.92 | – | 12.55 | 35.48 | – | – | – | – | – |
| Acanthite | Ag _{1.9} S | Mean | 2 | – | 86.61 | – | 13.39 | – | – | – | – | – | – |
| | | S.D. | | – | 1.58 | – | 1.58 | – | – | – | – | – | – |
| | | Min | | – | 85.49 | – | 12.27 | – | – | – | – | – | – |
| | | Max | | – | 87.73 | – | 14.51 | – | – | – | – | – | – |
| Cervelleite | Ag _{3.94} Te _{1.18} S | Mean | 6 | – | 70.00 | 24.71 | 5.29 | – | – | – | – | – | – |
| | | S.D. | | – | 1.58 | 1.87 | 0.51 | – | – | – | – | – | – |
| | | Min | | – | 67.05 | 23.36 | 4.55 | – | – | – | – | – | – |
| | | Max | | – | 71.70 | 28.40 | 5.85 | – | – | – | – | – | – |
| Early generation Galena | | Mean | 9 | – | – | – | 17.79 | 82.21 | – | – | – | – | – |
| | | S.D. | | – | – | – | 0.26 | 0.26 | – | – | – | – | – |
| | | Min | | – | – | – | 17.19 | 81.96 | – | – | – | – | – |
| | | Max | | – | – | – | 18.04 | 82.81 | – | – | – | – | – |
| Late generation Galena | | Mean | 7 | – | 1.21 | – | 14.58 | 84.28 | – | – | – | – | – |
| | | S.D. | | – | 0.84 | – | 1.45 | 1.55 | – | – | – | – | – |
| | | Min | | – | – | – | 12.93 | 81.64 | – | – | – | – | – |
| | | Max | | – | 2.31 | – | 16.46 | 86.19 | – | – | – | – | – |
| Sphalerite | | Mean | 27 | – | – | – | 33.23 | – | 56.90 | 9.34 | – | 0.46 | – |
| | | S.D. | | – | – | – | 0.67 | – | 0.76 | 0.38 | – | 0.25 | – |
| | | Min | | – | – | – | 32.57 | – | 53.89 | 8.62 | – | – | – |
| | | Max | | – | – | – | 36.07 | – | 57.93 | 10.13 | – | 0.82 | – |
| Sphalerite ^a | | Mean | 5 | – | – | – | 33.27 | – | 54.96 | 8.76 | – | 0.56 | – |
| | | S.D. | | – | – | – | 0.40 | – | 0.23 | 0.17 | – | 0.16 | – |
| | | Min | | – | – | – | 32.67 | – | 54.64 | 8.46 | – | 0.39 | – |
| | | Max | | – | – | – | 33.65 | – | 55.23 | 8.87 | – | 0.79 | – |
| Pyrite | | Mean | 7 | – | – | – | 52.32 | – | – | 47.10 | – | 0.06 | – |
| | | S.D. | | – | – | – | 0.41 | – | – | 0.32 | – | 0.05 | – |
| | | Min | | – | – | – | 51.61 | – | – | 46.46 | – | – | – |
| | | Max | | – | – | – | 52.73 | 1.22 | 0.63 | 47.52 | – | 0.11 | – |
| Chalcopyrite | | Mean | 4 | – | – | – | 34.39 | – | – | 31.06 | 34.39 | – | – |
| | | S.D. | | – | – | – | 0.19 | – | – | 0.46 | 0.25 | – | – |
| | | Min | | – | – | – | 34.21 | – | – | 30.68 | 34.06 | – | – |
| | | Max | | – | – | 0.68 | 34.61 | – | – | 31.73 | 34.66 | – | – |

^a Wavelength-dispersive spectrometer, others were analysis by energy spectrum; “–” lower than detection limits.

and are overprinted by late-stage Ag–Te–S phases (Fig. 2h). Microanalysis indicates mean compositions of 36.57% Bi, 42.81% Pb, 12.68% Te, and 7.95 wt% S. The calculated formula Bi_{2.12}Pb_{2.49}Te_{1.20}S₃ approximates to saddlebackite (Pb₂Bi₂Te₂S₃; Criddle and Stanley, 1993), or other Bi–Pb Te sulfides (Cook et al., 2007a). Its mineral species needs some further work to be sure.

4.1.6. Ag–Pb–Bi sulphosalts

The Ag–Pb–Bi–S minerals are present in minor quantities as amorphous textures, and occur as veinlets in sharp contact with early generation galena (Fig. 2i). They are dominated by Ag

(7.65 ± 0.24%), Pb (12.44 ± 0.13%), Bi (45.41 ± 1.1%) and S (34.50 ± 0.85%), and are deficient in Te (Table 1 and Appendix 1). The calculated formula is Pb_{2.15}Bi_{2.80}Ag_{0.91}S₅, with the formula simply expressed as Pb₂Bi₃AgS₅. In contrast with cannizzarite (Pb₃Bi₄S₉), bonchevite (PbBi₄S₇), cosalite (Pb₂Bi₂S₅), lillianite (Pb₃Bi₂S₆), Pb₆(Bi,Sb)₅S₁₇, heyrovskyite (Pb₆Bi₂S₉), and giessenite (Pb₅Bi₆S₁₇) (Criddle and Stanley, 1993), the studied mineral is more closely related to galenobismutite (PbBi₂S₄) with a content of 27.50% Pb, 55.48% Bi, and 17.02% S, and a significant minor amount of S (Criddle and Stanley, 1993). In fact, Ag–Pb–Bi–S minerals can be difficult or impossible to tell apart by probe analysis alone. They

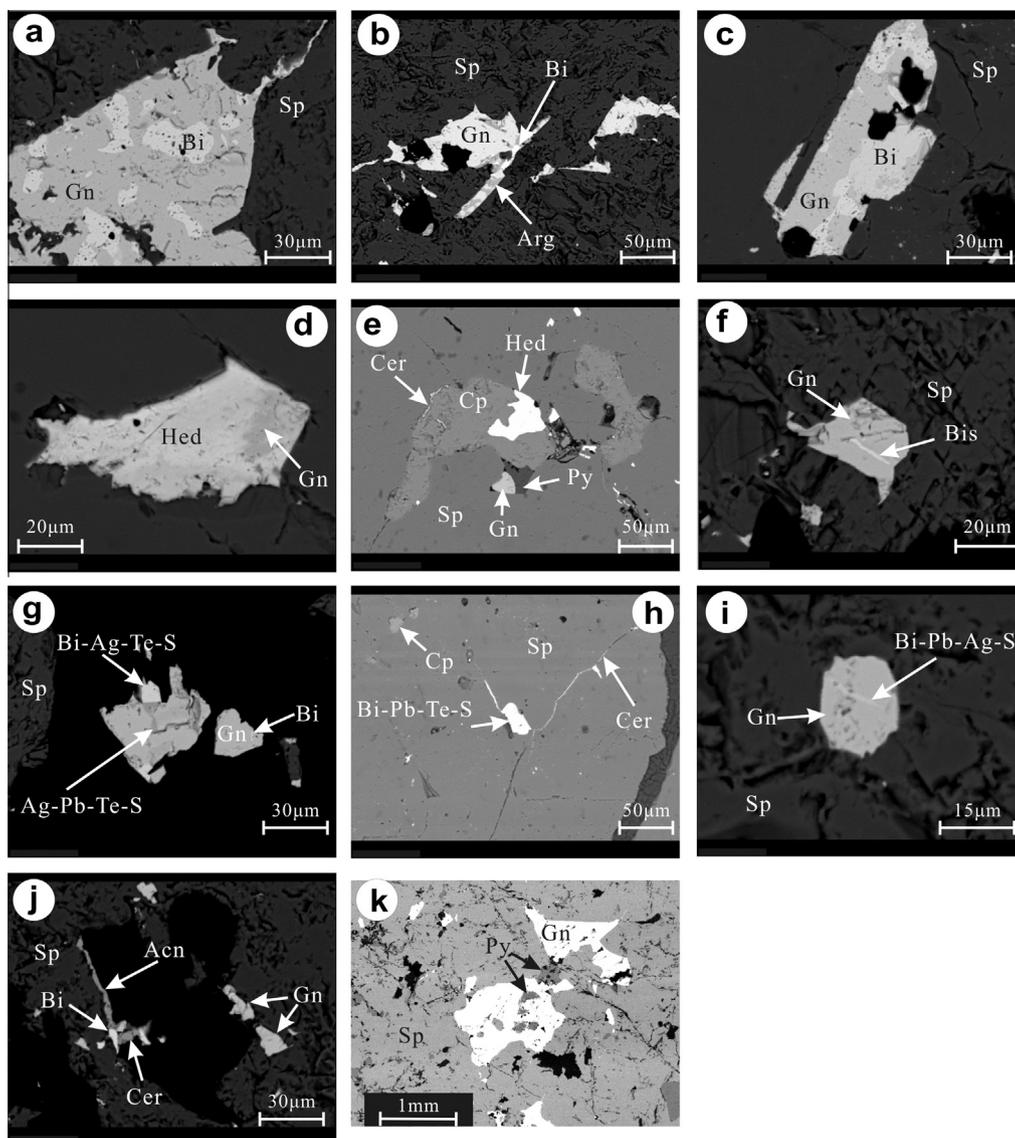


Fig. 2. Back scattered electron images of Bi minerals from the Dabaoshan Pb–Zn polymetallic deposit. (a) Native Bi, as infill veinlets along cracks (interstitial) in sphalerite, is replaced by late generation galena. Note an absence of Bi in the galena and sphalerite. (b) Native Bi occurs as infill veinlets along cracks or is interstitial in the sphalerite, corroded by late generation galena and acanthite. The galena and sphalerite are deficient in Bi and Ag. (c) Early generation galena is replaced by native Bi, with a scarcity of Bi and Ag in the galena and sphalerite. (d) Early generation galena corroded by hedleyite. (e) Chalcopyrite replaced by hedleyite, and cervelleite occurring as infill veinlets along fractures in the chalcopyrite and sphalerite. (f) Bismuthinite is present as veinlets within the early generation galena. (g) Native Bi occurring as veinlets in the early generation galena, and undefined Bi–Ag–Te–S minerals replaced by indeterminate Ag–Pb–Te–S minerals. (h) Undefined Bi–Pb–Te–S minerals occurring as overgrowths in vugs of sphalerite, is replaced by cervelleite as veinlets. (i) Early generation galena replaced by undefined Bi–Pb–Ag–S minerals as veinlets. (j) Veinlet overgrowths of native Bi in the interstices between sphalerite and gangue minerals, replaced by cervelleite and acanthite. (k) A coarse-grained and anhedral early generation galena with low Bi and Ag content. Bi, native bismuth; Hed, hedleyite; Aca, acanthite; Cer, cervelleite; Bis, Bismuthinite; Bi–Ag–Te–S, Bi–Ag–Te–sulfides (undefined mineral); Bi–Pb–Te–S, Bi–Pb–Te–sulfides (undefined mineral); Ag–Pb–Te–S, Ag–Pb–Te–sulfides (undefined mineral); Sp, Sphalerite; Gn, Galena; Py, Pyrite; Cp, Chalcopyrite.

often form solid solutions or are intergrown at the finest scale (Moëlo et al., 2008). It is suggested the mineral may be a member of the lillianite homologous series.

4.2. Silver minerals

Compared with other Pb–Zn deposits in China (e.g., Huizhe, Yunnan and Bainiuchang, up to 200 g/t and 92 g/t Ag respectively, Han et al., 2007; Liu et al., 2007), the lower average grade of sulfides from the Dabaoshan district is 61.87 g/t Ag (He and Song, 1990). Silver mostly occurs within independent minerals, and in addition to the Ag–Bi assemblages mentioned above, there are two other silver minerals present at Dabaoshan: argentite and Ag–Te–S minerals.

Acanthite occurs as anhedral grains or frequently as veinlets along cracks within the sphalerite, often overprinting early generation galena and native bismuth (Fig. 2b, j). This mineral is not the mineral of isometric system, and microprobe data show the presence of Ag (to $86.61 \pm 1.58\%$) and S ($13.39 \pm 1.58\%$), and an absence of Bi, Pb and Te (Table 1 and Appendix 1). The calculated formula is $Ag_{1.93}S_1$, which may be simply expressed as Ag_2S , which is generally consistent with the ideal value for acanthite (Ag_2S ; Wang et al., 1982; Cook et al., 2009b).

The Ag–Te–S assemblages occur as infill veinlets along grain boundaries between sphalerite and less frequently chalcopyrite, and contain mainly Ag, Te and S ($70.00 \pm 1.58\%$, $24.71 \pm 1.87\%$, $5.29 \pm 0.51\%$, respectively) (Table 1 and Appendix 1). The calculated formula is $Ag_{3.94}Te_{1.18}S$, which may be simply expressed as

Ag₄TeS. In contrast to silver tellurides such as empressite (AgTe, with 45.81% Ag, 54.91% Te; Cipriani, 2004) and hessite (Ag₂Te, with 62.42% Ag, 36.96% Te, and 0.24% Fe; Wang et al., 1982), the composition is same with cervelleite (Ag₄TeS; Criddle and Stanley, 1993; Cook and Ciobanu, 2003).

4.3. Distribution characteristics of Bi and Te in galena and sphalerite

Reflected light microscopy and microanalytical data indicate two periods of galena formation: early and late generation. The former is the most common, and was deposited during the main mineralization stage, and mainly occurs as coarse grains (0.1 mm × 0.2 mm to 0.7 mm × 1 mm), anhedral grains associated with sphalerite (Fig. 2k), or as partly anhedral disseminated textures in the gangue minerals (Fig. 2c, f). It is worth noting that no microinclusions were detected in this galena. Microprobe analysis indicates the presence of Pb (from 81.96% to 82.81%; mean 82.21%, *n* = 9) and S (from 17.19% to 18.04%; mean 17.79%, *n* = 9), and scarce Bi, Te and Ag (Table 1 and Appendix 1). Nevertheless, the late generation galena (Fig. 3), which formed during the late overprinting mineralization stage, is relatively abundant, and mostly occurs as anhedral grains along cracks in the sphalerite or as veinlets penetrating sphalerite and gangue minerals. Additionally, it is significantly finer-grained than the early generation galena, often replacing native Bi as inclusions, and was deposited after formation of the Bi minerals, which thus may be linked to the late-stage overprinting of the ore deposits. Microprobe analysis implies that in contrast to the early generation galena, late generation galena contains an elevated Pb content (to 84.28 ± 1.55%); relatively lower S content (14.58 ± 1.45%). In the energy spectra, there was no Bi or Te peak, and only occasional Ag (up to 2.31% in a single sample).

The sphalerite in the Dabaoshan deposit occurs as anhedral crystals, coexisting with the early stage galena, and is preserved as inclusions within the pyrite (Fig. 2k), often replaced by chalcopyrite (Fig. 2e). The energy spectra data are consistent with those of a wave spectrum (Table 1 and Appendix 1), and shows the presence of Zn (54.64–55.23%, mean 54.96%, *n* = 5) and S (32.67–33.65%, mean 33.27%, *n* = 5), a significant amount of Fe (8.46–8.87%, mean 8.76%, *n* = 5), and trace amounts of Cd and Pb. The composition is close to Fe-sphalerite, which forms at higher temperatures (Liu et al., 1984). Galena, sphalerite, chalcopyrite, and pyrite do not contain measurable Bi. Moreover, LA-ICP-MS analysis of sphalerite from Dabaoshan (Ye et al., 2011) indicates

that the Bi, Te, and Ag contents were lower than the analytical detection limits for these elements, suggesting extremely low concentrations of lattice-hosted Bi or Te in sphalerite.

5. Discussion

5.1. Genetic implications for Bi, Te and Ag

Generally, there is a close genetic relationship between Bi and Te in most deposits (Liu et al., 1984). Bismuth in nature often is hosted in gold deposits, and can be used as an indicator element for gold prospecting (Luo et al., 1993; Chen, 2001) for most global gold deposits (e.g. Tuomo and Randolph, 2005; Oberthür and Weiser, 2008), such as the Chinese examples at Jiaodong (Pan, 1994), Aletai Sarekuobu (Zhong et al., 2005), Qinling area (Mao et al., 2002), Kendekeke (Pan and Sun, 2003), Tongling (Ren et al., 2004), Baolun (Wang et al., 2006b) and Sarekoubu (Xu et al., 2008a). In addition, native bismuth has two modes of occurrence. First, it may form in relation to high temperature hydrothermal fluids, often coexisting with cassiterite, wolframite, bismuthinite, tourmaline and beryl, e.g., in most mid-high temperature magmatic hydrothermal deposits (Newberry, 1998; Liu et al., 1998; Huang et al., 2000; Barkov et al., 2008) and in pegmatitic deposits (Heinrich, 1946; Simmons, 2001). Second it may be found in reducing environments, as native bismuth associated with mid-high temperature hydrothermal minerals (e.g., galena and chalcopyrite) (Taylor, 1964; Wang et al., 1982; Liu and Bassett, 1986; Mou, 1999; Miller and Craig, 1997; Voudouris et al., 2008). Based on the paragenetic assemblages and mode of occurrence for native Bi, the Dabaoshan occurrence formed in the mid-temperature reduced environment, and is coarse grained, suggesting metastable conditions in the formation of Bi.

Tellurium belongs to the sulfur family elements, and is dispersed in the crust (Liu et al., 1984). It is strongly dispersed in high temperature conditions which show shows an affinity to oxygen, whereas it is concentrated in the lower mid-temperature condition (Wang et al., 1982) and shows a sulfur affinity. Te-minerals forms normally under extremely low *f*S₂ and high *f*Te₂ conditions (Chen et al., 1999). Some examples in China include the Dashuigou Te–Bi deposit in Sichuan province, the Guilaizhuang Te–Au deposit in Shandong Province, and the Dongping Te–Au deposit in Henan province (Qian et al., 2000; Cook et al., 2009a; Ciobanu et al., 2012).

Tellurides are another main mode of occurrence of Bi and Ag in the Dabaoshan deposit, such as hedleyite and other undetermined

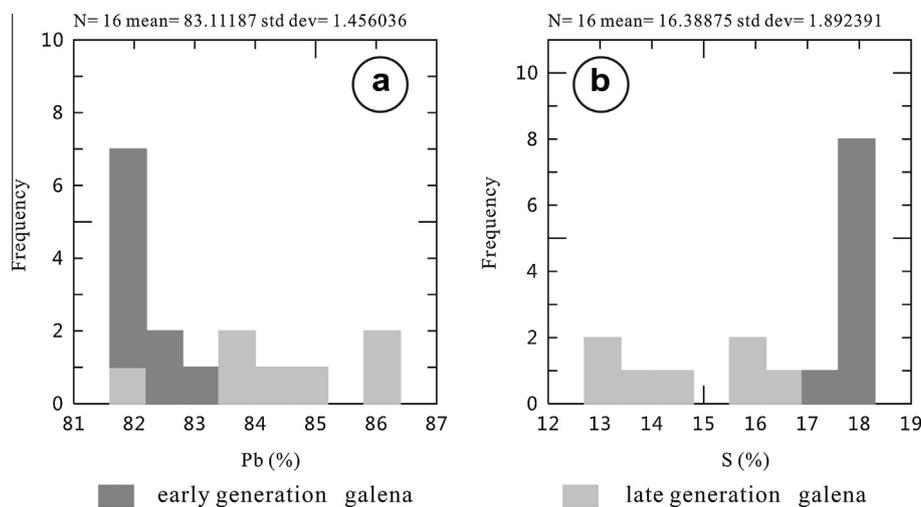


Fig. 3. Componential histogram figure of early and late generation galena.

minerals (e.g., Bi–Ag–Te–S, Bi–Pb–Te–S, Bi–Pb–Ag–S and Ag–Te–S). These minerals are often concentrated in lower mid-temperature deposits, with a formation temperature range of 266–312 °C for hedleyite (Elliot, 1965). Therefore, this mode of occurrence of Bi and Ag implies that the ore-forming fluid may be characterized as Te-rich and S-poor and develop in the lower mid-temperature environment during the mineralization stage. Bi belongs in the group VB elements in the periodic table with a relatively strong metallicity. In nature, Bi is marked by the presence of Bi^{3+} and, due to its resemblance to the electronic configuration of Pb^{2+} ; there is a close relationship between Bi^{3+} and Pb^{2+} . In determining the mode of occurrence of Bi in galena, one of the least understood issues with the greatest ramifications is whether substitution of Pb by Bi in the galena is isomorphic or present as tiny inclusions (Liu et al., 1984). Nevertheless, it is well known that galena is the predominate Bi-hosting mineral (Wang et al., 1982; Liu et al., 1984), e.g., as found in the Yinshan Pb–Zn deposit in Jiangxi province (Huang, 1999) and in the Haobugao Pb–Zn deposit in Mongolia (Huang, 2000). The sulfides, particularly galena, are rich in Bi, as seen in the products of the Yanshanian intermediate–acidic intrusion (marked by abundant Bi), which is not consistent with the results presented in this paper. Based on energy spectra analysis of galena, there is no Bi or Te peak in the early generation galena, indicating an extremely low Bi and Te content in these sulfides. It is suggested that in the main mineralization stage of formation of the Pb–Zn sulfides, the ore-forming fluids were extreme low Bi and Te concentration. In combination with mineragraphy and EPMA micro-textures, the Dabaoshan sulfides were precipitated before formation of the Bi and Ag minerals, and therefore may have been derived from multi-sources and experienced a multi-genesis. Furthermore, in comparison to the early generation galena, late generation galena has lower S content, higher Pb, Zn, Fe and Ag content, and is deficient in Bi and Te, indicating that the ore-forming fluids were Bi-, Te-, and S-poor in this stage.

Mineragraphy and microscopic identification revealed a paragenetic sequence of pyrite → sphalerite and early generation galena → chalcopyrite → native Bi and hedleyite (Bi_7S_3) → Bi–Ag–Te–S minerals and Bi–Pb–Ag–S assemblages → cervelleite (Ag_4TeS) and Ag–Pb–Te–S associations → acanthite (Ag_2S) → late generation galena.

The Bi and Ag minerals are mostly replaced by late generation galena, a coarse-grained crystal, or occur as infill veinlets along cracks and vugs in the sphalerite, indicating that this ore deposit was overprinted by Bi-, Te- and Ag-rich fluids accompanied by

related mineralization. In the relatively stable, early overprinting stage, the fluids were rich in Bi and Te, and poor in S. During a subsequent decrease in temperature during evolution of the ore-forming fluids, Ag, Pb and S were concentrated, at which time Bi and Te precipitated (Fig. 4). The sulfur may have been derived from early stage sulfides during overprinting.

5.2. The origin of Bi in the sulfides

The existing state of Bi indicates that its enrichment mechanism is different from that of the weathering zone in some Pb–Zn deposits (e.g. eastern Lachlan Fold Belt, NSW, Australia; Scott et al., 2001). Furthermore, the abundance of Bi in the crust is extremely low at 0.16×10^6 (Rudnick and Gao, 2005). Being of a larger ionic radius, it is possible that Ca^{2+} in the silicate minerals is substituted by Bi. Bi is frequently enriched in plagioclase-bearing rocks, e.g., intermediate and acid rocks as sources for Bi in some ore deposits (Liu et al., 1984). Bi enrichment of Pb–Zn deposits in China is mostly related to the Yanshanian–Himalayan granites, e.g., the Chaijiaying Pb–Zn deposit in Hebei (Huang et al., 1991); at Zhengcha, Jinling (Chen and Sun, 1995), and the Huangshaping and Baoshan Cu–Mo–Pb–Zn–Ag ore fields in Hunan (Zhong et al., 1997; Yang and Chen, 1998; Liao, 2009), the Yinshan Cu–Pb–Zn polymetallic deposit in Jiangxi (Liu, 2000); the Jiagang–Xueshan Wu–Mo–Bi polymetallic deposit in Xainza County, Tibet (Wang et al., 2007), and the skarn type Cu–Pb–Zn polymetallic deposit in the Bangong–Nujiang metallogenic belt (Zhao et al., 2010).

In the Dabaoshan ore area, the Devonian seafloor volcanic–sedimentary sequence is the ore-bearing stratum. It is high in Pb and Zn content, but extremely low in Bi content (Wang, 2006), which signifies that it cannot be the source for Bi in the ore deposit. As stated above, the Dabaoshan mine records two periods of intermediate–acid igneous activity, resulting in formation of larger scale secondary dacite–porphyry and granodiorite. The granodiorites are rich in Mo, and the abundance of Mo is 3–8 times that of the secondary dacite–porphyry, which is closely related to Mo mineralization in the northern of Dabaoshan mine (Wang, 2006; Wang et al., 2006a). On the other hand, the secondary dacite–porphyry is marked by enrichment of Bi (mean 15 ppm, $n = 248$, Wang et al., 2006a), higher ($n \times 10^2$ to $n \times 10^3$) than its concentration generally in intermediate–acid intrusions (0.01 ppm, Turekian and Wedepohl, 1961). At Dabaoshan, the Bi content is $n \times 10^3$ to $n \times 10^4$ times greater than crustal abundances, and 2–3 times greater than that of the granodiorite–porphyry (mean 6.9 ppm,

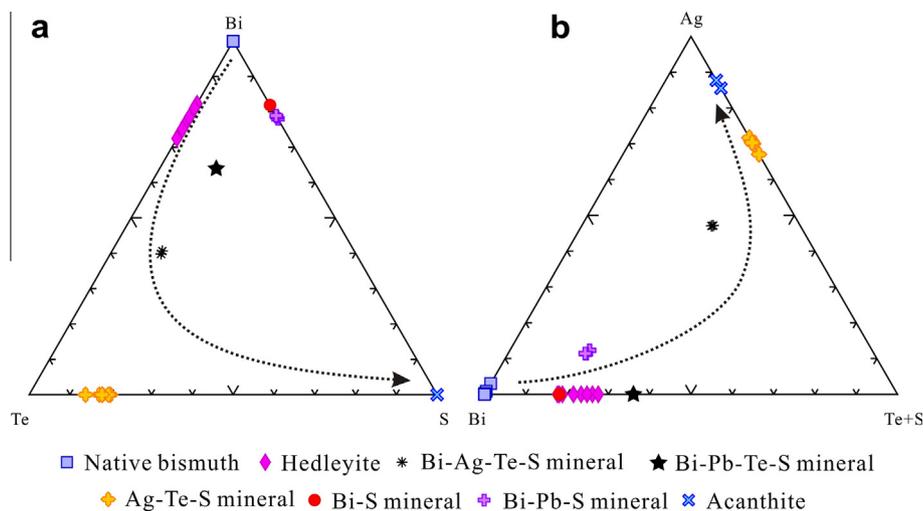


Fig. 4. Triangular plots for Bi–Te–S (a) and Ag–Bi–(Te+S) (b) of the Bi and Ag minerals occurring in the Dabaoshan mine district.

$n=99$). Therefore, it is suggested that the secondary dacite-porphphyry intruding Pb–Zn polymetallic orebodies might be the primary source for Bi in this ore district.

The Dabaoshan deposit undeniably records much evidence of syngenetic sedimentary geology and geochemistry (Chen, 1985; Ge and Han, 1986; Yang, 1997; Gu et al., 2007), whereas the overprinting of Dabaoshan deposit by the Yanshanian intermediate-acid intrusion cannot be ignored (Qiu, 1981; Deng et al., 2005; Song et al., 2007; Xu, 2008b). The overprinting not only resulted in formation of strong alteration of wall-rock (e.g., skarnization, tremolitization, actinolitization, chloritization, silicification, sericitization, calcinations, potassic alteration, and greisenization), but also caused injection of most of the metallogenic materials into the Devonian syngenetic sedimentary Pb–Zn polymetallic mineralization. This led to formation of complex multi-element assemblages during mineralization, including Fe, Cu, Pb, Zn, S, W, Mo, Sn, Ag, Au, Cd, Ga, Ge, Sb, Se, Te, Th, Tl, Nb, Ta, Re, Co, Ni and Mn. Because Bi and Te are generally lacking in sulfides which formed during the early mineralization stage, the enrichment of Bi, Te and Ag is attributed to the late Yanshanian secondary dacite-porphphyry intrusion event.

6. Conclusions

Based on the results presented herein, the following conclusions may be drawn:

- (1) At Dabaoshan, bismuth mainly occurs as discrete minerals enclosed by late-generation galena or as veinlets at the boundary of sulfides, and formed in the late main stage of formation of the Pb–Zn deposit. Bismuth speciation is diverse and includes native bismuth, tellurides, tellurosulfides, sulfides and sulfosalts; native bismuth and hedleyite are the most abundant species. In contrast to native Bi common in gold deposits, and native Bi derived from gasification of high-temperature hydrothermal fluids, the mode of occurrence of Bi in the Dabaoshan ore deposit is similar to lower-mid-temperature hydrothermal deposits.
- (2) The contents of Bi, Te, and Ag are extremely low in the sulfides (e.g., galena and sphalerite) that formed during the main Pb–Zn mineralization stage, and the enrichment of Pb, Zn, Bi, Ag, and Te can be interpreted as multi-sourced and multi-genetic. The Pb–Zn mineralization is not linked to the Yanshanian intermediate-acid intrusions.
- (3) Bi and Te are predominately derived from the late Yanshanian secondary dacite-porphphyry. During the intrusion of this porphyry, Bi and Te-rich ore-forming fluids migrated into fractures resulting in formation of sulfides, and corroding the Pb–Zn mineralization.
- (4) In the relatively stable early overprinting stage, the fluids were rich in Bi and Te, and poor in S. With a decrease in temperature during evolution of the ore-forming fluids, Ag and Pb became enriched, and up to the late overprinting stage, the concentration of S in the fluids increased, resulting in precipitation of Bi and Te. The origin of sulfur may be related to remobilization of the early stage sulfides during overprinting.

Acknowledgements

This research project was jointly supported by the National Natural Science Foundation of China (Grant No. 41173063) and the 12th 569 Five-Year Plan Project of State Key Laboratory of Ore-deposit Geochemistry, Chinese Academy of Sciences (SKLOGD-ZY125-02). We are greatly indebted to Chief Engineer

Liu Cong (Dabaoshan Mining Limited Company, Guangdong Province) who assisted with sampling. We thank Prof. Nigel J. Cook and the *Journal of Asian Earth Sciences* reviewer for their constructive comments on this manuscript, and Editor-in-Chief Irene Yao for her helpful suggestions.

Appendix A. Supplementary material

Supplementary data associated with this article can be found, in the online version, at <http://dx.doi.org/10.1016/j.jseaes.2013.12.006>. These data include Google maps of the most important areas described in this article.

References

- Barkov, A.Y., Martin, R.F., Shi, L., Lebarge, W., Fedortchouk, Y., 2008. Oscillator zoning in stanniferous hematite and associated W- and Bi-rich minerals from Canadian Creek, Yukon, Canada. *Can. Mineral.* 46, 59–72.
- Chen, H.S., 1985. Geochemical investigations on the lead, sulphur and oxygen isotopes of the Dabaoshan stratiform polymetallic deposit, northern Guangdong. *J. Yichang Inst. Geol. Miner. Resour.* 10, 111–121 (in Chinese with English abstract).
- Chen, D.F., Sun, S.Q., 1995. The main characteristics of minerals and their mineral associations in the Zhengcha lead–zinc deposit, Jilin province. *Geol. Rev.* 41, 52–60 (in Chinese with English abstract).
- Chen, C.H., Cao, Z.M., Hou, X.P., Shuai, D.Q., Tuo, Y.N., 1999. The distributive law and main minerogenic conditions of gold telluride deposits in the world. *J. Chengde Univ. Technol.* 26, 241–248 (in Chinese with English abstract).
- Chen, Y.C., Li, Z.N., Wu, R.S., 2001. Gold Deposits in China and its Metallogenic Regularity. Geological Publishing House, Beijing, p. 200, (in Chinese with English abstract).
- Ciobanu, C.L., Pring, A., Cook, N.J., Self, P., Jefferson, D., Dima, G., Melnikov, V., 2009. Chemical-structural modularity in the tetradymite group: a HRTEM study. *Am. Mineral.* 94, 517–534.
- Ciobanu, C.L., Birch, W.D., Cook, N.J., Pring, A., Grundler, P.V., 2010. Petrogenetic significance of Au–Bi–Te–S associations: the example of Maldon, central Victorian gold province, Australia. *Lithos* 116, 1–17.
- Ciobanu, C.L., Cook, N.J., Utsunomiya, S., Kogagwa, M., Green, L., Gilbert, S., Wade, B., 2012. Gold–telluride nanoparticles revealed in arsenic-free pyrite. *Am. Mineral.* 97, 1515–1518.
- Cipriani, C.E., 2004. AgTe, from the Empress-Josephine mine, Colorado, USA: composition, physical properties, and determination of the crystal structure. *Am. Mineral.* 89, 1043–1047.
- Cook, N.J., Ciobanu, C.L., 2003. Cerveleite, Ag₄TeS, from three localities in Romania, substitution of Cu, and the occurrence of the associated phase, Ag₂Cu₂TeS. *Neues Jahrbuch für Mineralogie-Monatshefte*, 321–336.
- Cook, N.J., Ciobanu, C.L., Stanley, C.J., Paar, W.H., Sundblad, K., 2007a. Compositional data for Bi–Pb tellurosulfides. *Can. Mineral.* 45, 417–435.
- Cook, N.J., Ciobanu, C.L., Wagner, T., Stanley, C.J., 2007b. Minerals of the system Bi–Te–Se–S related to the tetradymite archetype: review of classification and compositional variation. *Can. Mineral.* 45, 665–708.
- Cook, N.J., Ciobanu, C.L., Mao, J.W., 2009a. Textural control on gold distribution in As-free pyrite from the Dongping, Huangtuliang and Hougou gold deposits, North China Craton, (Hebei Province, China). *Chem. Geol.* 264, 101–121.
- Cook, N.J., Ciobanu, C.L., Spry, P.G., Voudouris, P., 2009b. Understanding gold–(silver)–telluride–(selenide) mineral deposits. *Episodes* 32, 249–263.
- Criddle, A.J., Stanley, C.J., 1993. Quantitative Data File for Ore Minerals, third ed. Chapman & Hall Publishing House, London, 635p.
- Deng, J., Yang, L.Q., Sun, Z.S., Wang, J.P., Wang, Q.F., Cheng, X.M., Zhou, Y.H., 2005. Late-paleozoic fluid systems and their ore-forming effects in the Yuebei basin, China. *Acta Geol. Sinica* 79, 673–687.
- Drummond, S.E., Ohmoto, H., 1985. Chemical evolution and mineral deposition in boiling hydrothermal system. *Econ. Geol.* 87, 126–147.
- Elliot, R.P., 1965. Constitution of Binary Alloys (First Supplement). McGrawHm Book Co. Inc. Press, New York, p. 877.
- Francis, C.A., Criddle, A.J., Stanley, C.J., Lange, D.E., Shieh, S., Francis, J.G., 1992. Buckhornite, AuPb₂BiTe₂S₃, a new mineral species from Boulder County, Colorado, and new data for aikinite, tetradymite and calaverite. *Can. Mineral.* 30, 1039–1047.
- Ge, C.H., Han, F., 1986. Submarine volcanic hydrothermal sedimentary origin of the Dabaoshan iron and polymetallic sulfide deposit. *Miner. Deposits* 5, 1–12 (in Chinese with English abstract).
- Gu, J.Y., Wu, Q.Y., Liao, X.P., 1984. Dabaoshan continental sub-volcanic and volcanic activities and the primary investigation on genesis of ore deposit. *Geol. Prospect.* 19, 1–8 (in Chinese with English abstract).
- Gu, L.X., Zaw, K., Hu, W.X., Zhang, K.J., Ni, P., He, J.X., Xu, Y.T., Lu, J.J., Lin, C.M., 2007. Distinctive feature of Late Palaeozoic massive sulphide deposits in South China. *Ore Geol. Rev.* 31, 107–138.

- Han, R.S., Liu, C.Q., Huang, Z.L., Chen, J., Ma, D.Y., Lei, L., Ma, G.S., 2007. Geological features and origin of the Huize carbonate-hosted Zn–Pb–(Ag) District, Yunnan, South China. *Ore Geol. Rev.* 31, 360–383.
- He, W.T., Song, Y.Z., 1990. Metallogenic regular investigation on gold and silver associated with ore minerals in the southern Dabaoshan Pb–Zn deposit, Qujiang, Guangdong. *Guangdong Non-ferr. Met. Geol.* 2, 14–21 (in Chinese with English abstract).
- Heinrich, E.W., 1946. Bismuth minerals in Colorado and New Mexico pegmatites. *Geol. Soc. Am. Bull.* 2, 1165.
- Huang, S., 1999. The mode of occurrence of Bi in the Yinshan Pb–Zn deposit, Jiangxi and its synthesis evaluation. *J. Guilin Inst. Technol.* 19, 40–46 (in Chinese with English abstract).
- Huang, S.J., Zeng, Y.C., Jia, G.X., Chen, Y.R., 1987. On the genesis of Dabaoshan polymetallic deposit in Guangdong province, China. *Geochimica* 16, 27–35 (in Chinese with English abstract).
- Huang, D.H., Ding, X.S., Wu, C.Y., 1991. Mineral characteristics and occurrence of gold, silver and bismuth of the Caijiaying leadzinc–silver deposit, Hebei province. *Acta Geol. Sinica* 65, 127–140 (in Chinese with English abstract).
- Huang, Y.H., Yue, S.Q., Qin, S.Y., Deng, C.J., Yang, J.M., Zhou, X.Z., Zhou, Z., 2000. Chinese Journal of Minerals (No. 1) – Natural Element Simple Substance and its Compound Minerals. Geological Publishing House, Beijing, p. 474, (in Chinese).
- Liao, T.D., 2009. Geological conditions of Cu–Mo–Pb–Zn–Ag deposit and prospecting prediction in the western Baoshan mine. *Hunan Nonferr. Met.* 25, 1–7 (in Chinese with English abstract).
- Liu, S.X., 2000. Process mineralogy of Cd, Ga, In and Bi in the Yinshan Cu–Pb–Zn polymetallic ore fields. *Hunan Nonferr. Met.* 16 (13–14), 45 (in Chinese with English abstract).
- Liu, L.G., Bassett, W.A., 1986. Elements, oxides and silicates. *High Pressure Phases with Implications for the Earth's Interior*. Oxford University Press, New York, p. 250.
- Liu, Y.J., Cao, L.M., Liu, Z.L., 1984. *Elementary Geochemistry*. Geological Publishing House, Beijing, p. 548, (in Chinese).
- Liu, H.Q., Yang, S.Y., Zhang, X.L., Chen, C.J., 1985. A preliminary study on the genesis of the Dabaoshan polymetallic deposit in northern Guangdong. *Acta Geol. Sinica* 1, 47–60 (in Chinese with English abstract).
- Liu, Y.M., Lu, H.Z., Wang, C.L., Xu, Y.Z., Kang, W.Q., Zeng, T., 1998. On the ore-forming conditions and ore-forming model of the superlarge multimetal deposit in Shizhuyuan. *Sci. China (Ser. D)* 41, 503–512.
- Liu, J.S., Zhang, H.P., Ouyang, Y.F., Zhang, C.H., 2007. Bainiuchang super-large silver–polymetallic ore deposit related to granitic magmatism in Mengzi, Yunnan. *J. Central South Univ. Technol.* 14, 568–574.
- Luo, Z.K., Guan, K., Yu, M.C., 1993. Overview of Gold Deposits in China. Tianjin Technological Publishing House, Tianjin, p. 308, (in Chinese).
- Mao, J.W., Goldfarb, R.J., Zhang, Z.W., Xu, W.Y., Qiu, Y.M., Deng, J., 2002. Gold deposits in the Xiaqingling–Xiong'er shan region, Qinling Mountains, Central China. *Miner. Deposita* 37, 306–325.
- Miller, J.W., Craig, J.R., 1997. Ore minerals of the Cofer volcanogenic massive sulfide deposit, Louisa County, Virginia. *Can. Mineral.* 35, 1465–1483.
- Moëlo, Y., Makovicky, E., Mozgova, N.N., Jambor, J.L., Cook, N.J., Pring, A., Paar, W., Nickel, E.H., Graeser, G., Karup-Møller, S., Balić-Žunić, T., Mumme, W.G., Vurro, V., Topa, D., Bindi, L., Bente, K., Shimizu, M., 2008. Sulfosalt systematics: a review. Report of the sulfosalt sub-committee of the IMA commission on ore mineralogy. *Eur. J. Mineral.* 20, 7–46.
- Mou, B.L., 1999. *Elementary Geochemistry*. Peking University Publishing House, Beijing, p. 227, (in Chinese).
- Newberry, R.J., 1998. W- and Sn-Skarn deposits: a 1998 status report. In: Lenz, D.R. (Ed.), *Mineralized Intrusion-Related Skarn Systems*, vol. 26. Mineralogical Association of Canada short Course Series, pp. 289–336.
- Oberthür, T., Weiser, T.W., 2008. Gold–bismuth–telluride–sulfide assemblages at the Viceroy Mine, Harare–Bindura–Shamva greenstone belt, Zimbabwe. *Mineral. Mag.* 72, 953–970.
- Pan, Y.C., 1994. Findings of Bi-bearing opaque minerals of the gold deposit in the Jiaodong area. *Gold Geol. Technol.* 39, 80–83 (in Chinese with English abstract).
- Pan, T., Sun, F.Y., 2003. The mineralization characteristic and prospecting of Kendekeke Co–Bi–Au deposit in Dunkunlun, Qinhai province. *Geol. Prospect.* 39, 18–22 (in Chinese with English abstract).
- Qian, H.D., Chen, W., Xie, J.D., Huang, J., 2000. A review of tellurium minerals. *Geol. J. China Univ.* 6, 178–187 (in Chinese with English abstract).
- Qiu, S.Q., 1981. A preliminary study on the genesis of the Dabaoshan stratiform polymetallic deposit. *Geol. Rev.* 27, 333–340 (in Chinese with English abstract).
- Ren, Y.S., Liu, L.D., Wang, X.Z., Chen, G.H., 2004. A study on the relationship between bismuth minerals and gold mineralization in skarn gold deposits in Shizishan orefield. *J. Mineral. Petrol.* 24, 41–45 (in Chinese with English abstract).
- Rudnick, R.L., Gao, S., 2005. Composition of the continental crust. In: Rudnick, R.L., (Ed.), *The Crust. Treatise on Geochemistry*, vol. 3, pp. 1–64.
- Scott, K.M., Ashley, P.M., Lawie, D.C., 2001. The geochemistry, mineralogy and maturity of gossans derived from volcanogenic Zn–Pb–Cu deposits of the eastern Lachlan Fold Belt, NSW, Australia. *J. Geochem. Explor.* 72, 162–191.
- Simmons, W.B., Webber, K.L., Falster, A.U., 2001. Tourmaline from the Malkhanskiy pegmatite district. *Mineral. Record* 32, 44.
- Song, S.M., Hu, K., Jian, S.Y., Li, K., 2007. The He–Ar–Pb–S isotope tracing on ore-forming fluid in Dabao hill polymetallic deposit, north Guangdong. *Contrib. Geol. Miner. Resour. Res.* 22 (87–92), 99 (in Chinese with English abstract).
- Taylor, S.R., 1964. Abundance of chemical elements in the continental crust: a new table. *Geochim. Cosmochim. Acta* 28, 1273–1285.
- Tu, G.C., Gao, Z.M., Hu, R.Z., Zhang, Q., Li, C.Y., Zhao, Z.H., Zhang, B.G., 2003. *Geochemistry and Mineralization Mechanism of Dispersed Elements*. Geology Publishing House, Beijing, p. 424, (in Chinese).
- Tuomo, O.T., Randolph, A.K., 2005. Gold enrichment and the Bi–Au association in pyrrhotite-rich massive sulfide deposits, Escanaba Trough, Southern Gorda Ridge. *Econ. Geol.* 100, 1135–1150.
- Turekian, K.K., Wedepohl, K.H., 1961. Distribution of the elements in some major units of the earth's crust. *Geol. Soc. Am. Bull.* 72, 175–192.
- Voudouris, P., Melfos, V., Spry, P.G., Bonsall, T.A., Tarkian, M., Solomos, Ch., 2008. Carbonate-replacement Pb–Zn–Ag±Au mineralization in the Kamariza area, Lavrion, Greece: mineralogy and thermochemical conditions of formation. *Mineral. Petrol.* 94, 85–106.
- Wang, J.X., 2006. Geological characteristics and ore prospecting orientation of lead zinc polymetallic deposit in south Dabaoshan, Guangdong. *Miner. Resour. Geol.* 20, 142–146 (in Chinese with English abstract).
- Wang, P., Pan, Z.L., Weng, L.B., 1982. *Systematic Mineralogy*, vol. I. Geological Publishing House, Beijing, p. 666, (in Chinese).
- Wang, D.B., Liang, J.G., Lin, Y., 2006a. The genesis of Dabaoshan Cu–Pb–Zn polymetallic deposit. *Dabaoshan Technol.* 31, 10–13 (in Chinese).
- Wang, P.A., Kaneda, H., Ding, S.J., Zhang, X.W., Liao, X.J., Dong, F.X., Li, Z.J., Liu, X.C., Lai, Y., 2006b. Geology and mineralogy of the Baolun hydrothermal gold deposit in the Hainan Island, South China. *Resour. Geol.* 56, 157–166.
- Wang, Z.H., Wu, X.Q., Wang, K.Q., Yu, W.Q., Huang, H., Ma, D.X., 2007. Stable isotope and ore genesis of Jiagangxueshan W–Mo–Bi polymetallic deposit, Shenzha county, Tibet. *Geol. Prospect.* 43, 6–10 (in Chinese with English abstract).
- Wang, L., Hu, M.G., Yang, Z., Chen, K.X., Xia, J.L., 2010. Geochronology and its geological implications of LA-ICP-MS zircon U–Pb dating of granodiorite porphyries in Dabaoshan polymetallic ore deposit, north Guangdong province. *Earth Sci. (J. China Univ. Geosci.)* 35, 175–185 (in Chinese with English abstract).
- Xu, J.H., Ding, R.F., Xie, Y.L., Zhong, C.H., Shan, L.H., 2008a. The source of hydrothermal fluids for the Sarekoubo gold deposit in the southern Altai, Xinjiang, China: evidence from fluid inclusions and geochemistry. *J. Asian Earth Sci.* 32, 247–258.
- Xu, W.X., Li, H., Chen, M.Y., Huang, D.X., Zhang, F.T., Wang, L.M., 2008b. Isotope evidence of material sources of the Dabaoshan polymetallic deposit. *Acta Geosci. Sinica* 29, 684–690 (in Chinese with English abstract).
- Yang, Z.Q., 1997. Origin of the Dabaoshan massive sulfide deposit: Devonian sea-floor thermal events. *Geol. Miner. Resour. South China* 4, 7–17 (in Chinese with English abstract).
- Yang, G.C., Chen, Z.Q., 1998. Alteration of wallrocks and the mineralization zoning features in Baoshan copper molybdenum lead zinc silver mineralization field. *Miner. Resour. Geol.* 12, 96–100 (in Chinese with English abstract).
- Ye, L., Cook, N.J., Ciobanu, C.L., Liu, Y.P., Zhang, Q., Liu, T.G., Gao, W., Yang, Y.L., Danyushevskiy, L., 2011. Trace and minor elements in sphalerite from base metal deposits in South China: a LA-ICPMS study. *Ore Geol. Rev.* 39, 188–217.
- Zhao, Y.Y., Liu, Y., Wang, R.J., Cui, Y.B., Song, L., Lü, N., Qu, X.M., 2010. The discovery of the bismuth mineralization belt in the Bangong Co–Nujiang metallogenic belt of Tibet and its adjacent areas and its geological significance. *Acta Geosci. Sinica* 31, 183–193 (in Chinese with English abstract).
- Zhong, Z.C., Deng, S.H., Wang, L.H., Gu, X.P., 1997. Association of silver mineralization in the Huangshaping lead zinc deposit. *Miner. Resour. Geol.* 11, 46–52 (in Chinese with English abstract).
- Zhong, C.H., Xu, J.H., Ding, R.H., Mao, Q., Xie, Y.L., 2005. Native bismuth in Sarekoubo gold deposit and its relation to gold mineralization. *Bull. Mineral. Petrol. Geochim.* 24, 130–134 (in Chinese with English abstract).